

PAPER • OPEN ACCESS

Mineral Detection from Hyperspectral Images Using a Spatial-Spectral Residual Convolution Neural Network

To cite this article: Hao Zeng *et al* 2021 *J. Phys.: Conf. Ser.* **1894** 012104

View the [article online](#) for updates and enhancements.



240th ECS Meeting

Digital Meeting, Oct 10-14, 2021

We are going fully digital!

Attendees register for free!

REGISTER NOW



Mineral Detection from Hyperspectral Images Using a Spatial-Spectral Residual Convolution Neural Network

Hao Zeng^{1,a}, Xiaoqing Han^{2,b}, Qingjie Liu^{*3,c}

¹School of Computer Science and Engineering, Beihang University, Beijing, China
Hangzhou Innovation Institute, Beihang University, Hangzhou, China

²Beijing Research Institute of Uranium Geology, Beijing, China

³School of Computer Science and Engineering, Beihang University, Beijing, China
Hangzhou Innovation Institute, Beihang University, Hangzhou, China

^a2454286244@qq.com, ^b1613739468@qq.com, ^cqingjie.liu@buaa.edu.cn

Abstract. Mineral detection from hyperspectral images is an interesting yet challenging research topic in the remote sensing community. Although many efforts have been put into this field, mineral detection is still far from solved, because compositions of minerals are very complex. The features of an interested mineral are very hard to be distinguished from others. In this paper, we attack this problem by introducing recently developed deep learning techniques. Beyond the spectral feature, considering that minerals coexist with each other, which could be regarded as a piece of special context information and thus can be captured by a spatial convolutional neural network (CNN), we design a CNN architecture that is able to exploit both spatial and spectral features of minerals. We test the proposed network on Indiana Pines dataset and a large-scale hyper-spectral image, the results demonstrate that the proposed method is good at representing both spatial and spectral information of hyper-spectral images and it can successfully detect minerals from hyperspectral images.

1. Introduction

Mineral detection from hyper-spectral images has been attracting increasing attention from both academic and industrial communities. Many techniques have been developed in the past decades, such as spectral similarity measure (SSM), spectral feature fitting (SFF) and mixed pixel decomposition (MPD). SSM identifies minerals by matching the ideal spectral curves of the minerals to the spectral data. Its results are robust to the atmosphere, but is easily affected by the mixed pixels. SFF is a method based on spectral absorption peaks. It can distinguish different minerals however may perform unstable when signal-to-noise ratios of the hyper-spectral data are large. MPD can separate mixed mineral effectively, but the pure pixel is hard to obtain. These methods only care about the spectral information, ignore the spatial information from neighbor pixels. Considering that, minerals always come together, we can use this information to help us to identify minerals from multi-spectral data. This co-existence relation can be considered as a spectral spatial or context information. Thus, exploring both spectral and spatial information of minerals is helpful for mineral recognition. Recently, deep learning techniques, such as deep belief networks [1], convolutional neural networks (CNNs) have made great progress and have been successfully applied in various fields of remote sensing, for example object detection [2-5], hyper-spectral image classification [4-11]. In this paper, we utilize CNN to capture the spatial and spectral information of hyper-spectral images (HSI) for mineral detection task.



Generally, there are two ways to learn the spatial-spectral features in deep learning methods. One way is dividing images into small patches and feeding them into CNNs to learn the spatial-spectral features, for example the 3D-CNN. Zhong et al. [6] proposed a 3D-CNN model that takes 3-D cube as input and jointly learns spatial and spectral features for HSI classification. This method reaches a high precision. However, under the same number of layers condition, 3-D CNNs require much more computation and parameters than 2-D CNNs. Another way is extracting spectral and spatial features separately and then fusing them to obtain the spatial-spectral representation. Xu et al. [8] proposed a spectral spatial unified network for hyper-spectral image classification, in which PCA was applied to obtain spatial information and spectral vectors are utilized to extract spectral information. Although good performance can be achieved, this method does not fully benefit from end-to-end training. Inspired by these progresses in hyper-spectral image classification, we develop an end-to-end CNN architecture for mineral detection in hyper-spectral images. Our method can

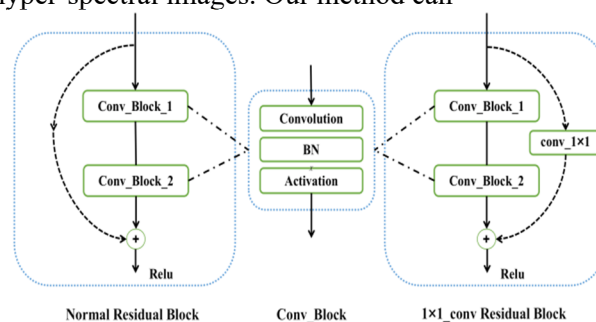


Figure.1 Building block of our model. The left is a classical residual block while the right one is the block used in this paper. We use 1×1 residual block to better extract spectrum information.

effectively extract spatial and spectral features and works well for classification task as well as mineral detection task.

This paper is organized as follows: In section 2, we introduce the proposed spatial-spectral residual network for mineral detection. Section 3 is dedicated to the experiments and discussions. In section 4, we draw a brief conclusion.

2. Methodology

In this section, we introduce our mineral detection method based on residual network. We firstly describe the details of the building block used in our model, then we introduce the model designed for mineral detection.

2.1. Residual Block

In the deep learning era, neural networks are designed to have much deeper layers because they will give much better performance than shallow ones. However, one of the major problems faced by deep neural networks is that it is very difficult to optimize the networks due to the gradient vanishing/exploding problem. The milestone method to solve this is the residual neural network [14]. He et al. [14] designed a residual block by adding a skip connection from the input to the output of a so-called plain convolutional unit. During training, the gradient information could back propagate smoothly without vanishing or exploding, thus enabling fast training and convergence.

Considering that, we intend to exploit both spatial and spectral features of hyperspectral image. Instead of utilizing the aforementioned residual block to build our network, we choose the block which its skip connection inserted by 1×1 Conv layer, as shown on the right side of Fig. 2. This 1×1 Conv path serves as a spectral feature extractor. And the stacked Conv layers act as a spatial feature extractor. Finally, the addition operation fuses the spatial and the spectral features of the images. The detailed structure of the building block is shown on the right side of Fig. 2.

2.2. Model Architecture

The network structure is shown in Fig. 1, which is simply comprised of four blocks and three fully connected (FC) layers. The four residual blocks in this model are allocated to accomplish features extraction task, and the FC layer with Softmax output performs mineral identification.

3. Experiments

In this section, we present experiments to valid the effectiveness and superiority of the proposed model to detect mineral.

3.1. Dataset

The experiments are conducted on two hyperspectral datasets. The first one is the Indian Pines dataset. This dataset was acquired by the Airborne Visible/Infrared Imaging Spectrometer (AVIRIS) sensor over the Indian Pines test site in north-western Indiana in 1992. The original data contain 220 spectral bands, ranging from 0.4 to 2.5 μm . After removing the bands covering the region of water absorption, we obtain the corrected data which has 200 bands. And there are 17 classes are annotated. The ground truth of this dataset is randomly separated into two equal parts, one was used as training data and the other for testing.

The second dataset was acquired over a mining area in Liuyuan, Gansu Province, China by Shortwave infrared Airborne Spectrographic Imager (SASI) imaging system in 2005. There are 12 adjacent strips in Liuyuan dataset, each of which was acquired by an airborne SASI sensor. The spatial resolution of the data is 2.0m. There are 101 bands in the dataset, and the spectrum curve covers a range of 950-2450nm. The mining area mainly contains 7 minerals: Dolomite, Calcite, High alumina Sericite, Medium alumina Sericite, Chlorite, Serpentine and Hornblende. All the minerals are verified through laborious ground investigations. And we label the investigation results (Fig. 3) on the Liuyuan data to generate training samples. Because the spectrums of the seven minerals have a good discrimination in the last 29 bands, we choose the last 29 spectral bands as the final dataset.

3.2. Settings

Before training, the data are normalized to have $[0, 1]$ distribution. For each mineral pixel identified by ground investigation, we crop its 3×3 neighbor patch to form a training sample. We use cross entropy loss and ADAM [16] to optimize our model. The learning rate used in both of the two experiments is set as 0.0005. Kernel sizes of the first two residual blocks are set as 2×2 (except the 1×1 shortcut convolution), and 1×1 for the other two residual blocks.

In order to eliminate the randomness of the selected training samples, we conducted 10 model training experiments. In testing phase, we calculate the overall

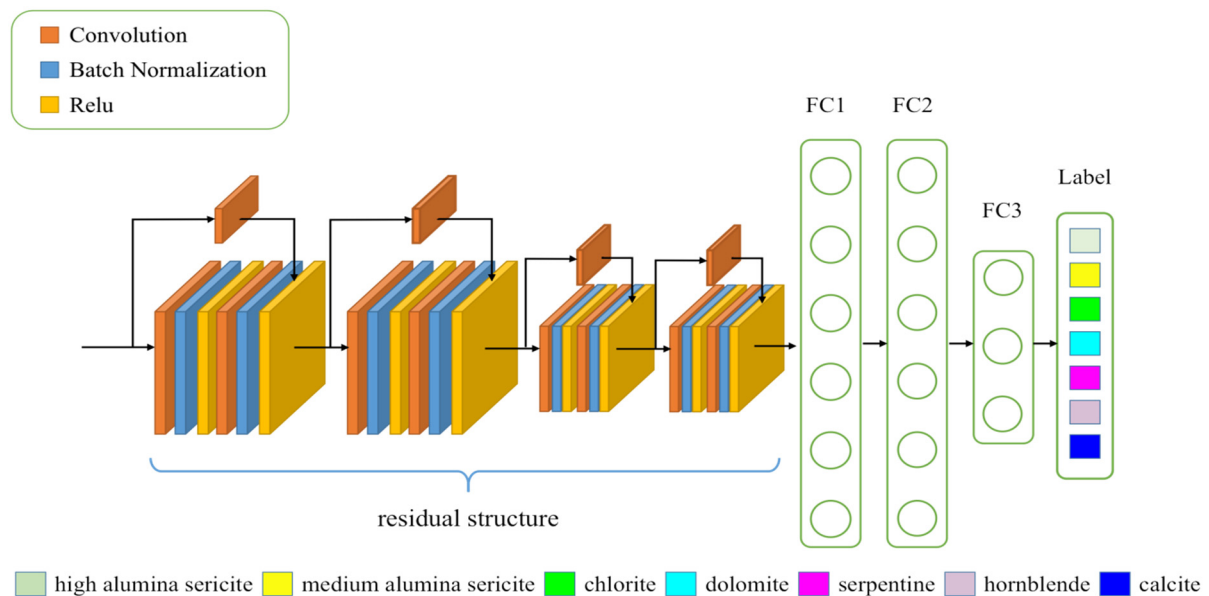


Figure.2 The network architecture of the proposed method

Table.1 Classification Results Of Different Approaches On The Indian Pine Dataset

ACC	APPROACHES					
	<i>TDBN-LR</i> [1]	<i>2D-CNN</i> [7]	<i>R-VCANet</i> [10]	<i>DFFN</i> [8]	<i>Res-1(direct)</i>	<i>Res-2(1×1 conv)</i>
OA(%)	91.34±0.26	95.97±0.09	97.90±0.32	98.52±0.23	96.27±0.93	98.73±0.35
AA(%)	89.70±0.34	93.23±0.76	97.91±0.58	98.32±0.32	96.84±1.23	98.80±0.41
Kappa	0.9013±0.0000	0.9540±0.0012	0.9760±0.0037	0.9769±0.0069	0.9578±0.0154	0.9835±0.0061

accuracy (OA), average accuracy (AA), and Kappa (K) coefficient to evaluate the performance of the proposed and the comparison methods. On the Indian Pines dataset, we compare our method to four deep learning based HSI classification approaches: DBN-LR [1], 2D-CNN [9], R-VCANet [15] and DFFN [10]. In addition, we also use the original residual network (Res-1 in Table 1) with direct connection shortcut as a baseline method. And the backbone of network is same to our model.

On the Liuyuan mineral dataset, we compare our method to mixture tuned matched filtering (MTMF), a widely used mineral recognition method.

3.3. Results

Table 1 illustrates quantitative results of the proposed and other five methods on the Indian Pines dataset. It can be seen the proposed method achieves the best results in terms of all evaluate metrics. The results show that our model can achieve a promising level in the task of hyperspectral classification.

The mineral detection result of the proposed method is shown in Fig. 3. Since the image is too large to see details, we crop a sub region from Liuyuan. The results are shown in Fig. 4. The results obtained by MTMF are distributed sparsely on the image, while our method is consistent with the ground investigation.

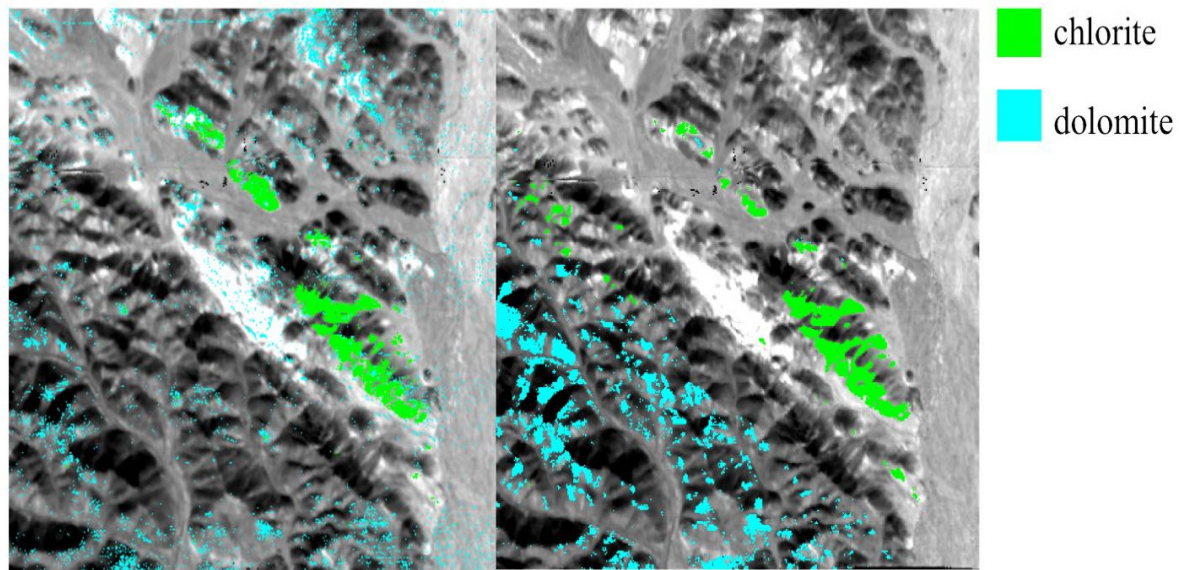


Figure.3 Mineral detection results of the proposed model on the Liuyuan data. There are seven minerals in the image. Liuyuan data is stitched by 12 strips and covers about 500km^2 . The colored dots are the regions rich in minerals and also the regions we conduct surface investigation.

4. Conclude

In this paper, we have proposed a mineral detection model which can extract effective spatial and spectral information, effectively. Experiment results demonstrate that our model can achieve higher accuracy compared to the other ways of fusing spatial-spectral features. Eventually, we apply our model to actual mineral RS dataset, the result shows deep learning method is more feasible than traditional algorithm in mineral detection.

Acknowledgement

* indicates Corresponding author. The work was supported by the High-resolution aerial gamma spectrometry and airborne imaging spectrometry technology resources exploration (2017YFC0602104), and Deep resources exploration and exploitation Key Project, National Key research and development plan.

References

- [1] Yushi Chen, Xing Zhao, and Xiuping Jia, "Spectral-spatial classification of hyperspectral data based on deep belief network," *IEEE Journal of Selected Topics in Applied Earth Observations and Remote Sensing*, vol. 8, no. 6, pp. 2381–2392, 2015.
- [2] Wei Li, Guodong Wu, and Qian Du, "Transferred deep learning for anomaly detection in hyperspectral imagery," *IEEE Geoscience and Remote Sensing Letters*, vol. 14, no. 5, pp. 597–601, 2017.
- [3] Konstantinos Makantasis, Konstantinos Karantzalos, Anastasios Doulamis, and Konstantinos Loupos, "Deep learning-based man-made object detection from hyperspectral data," in *International Symposium on Visual Computing*. Springer, 2015, pp. 717–727.
- [4] Cheng, Gong, and Junwei Han. "A survey on object detection in optical remote sensing images." *International Society for Photogrammetry and Remote Sensing Journal of Photogrammetry and Remote Sensing* 117 (2016): 11-28.
- [5] Li, Ke, et al. "Object detection in optical remote sensing images: A survey and a new benchmark." *International Society for Photogrammetry and Remote Sensing Journal of Photogrammetry and Remote Sensing* 159 (2020): 296-307.

- [6] Zilong Zhong, Jonathan Li, Zhiming Luo, and Michael Chapman, "Spectral-spatial residual network for hyperspectral image classification: A 3-d deep learning framework," *IEEE Transactions on Geoscience and Remote Sensing*, vol. 56, no. 2, pp. 847–858, 2017.
- [7] Wenzhi Zhao and Shihong Du, "Spectral-spatial feature extraction for hyperspectral image classification: A dimension reduction and deep learning approach," *IEEE Transactions on Geoscience and Remote Sensing*, vol. 54, no. 8, pp. 4544–4554, 2016.
- [8] Yonghao Xu, Liangpei Zhang, Bo Du, and Fan Zhang, "Spectral-spatial unified networks for hyperspectral image classification," *IEEE Transactions on Geoscience and Remote Sensing*, vol. 56, no. 10, pp. 5893–5909, 2018.
- [9] Jun Yue, Wenzhi Zhao, Shanjun Mao, and Hui Liu, "Spectral-spatial classification of hyperspectral images using deep convolutional neural networks," *Remote Sensing Letters*, vol. 6, no. 6, pp. 468–477, 2015.
- [10] Weiwei Song, Shutao Li, Leyuan Fang, and Ting Lu, "Hyperspectral image classification with deep feature fusion network," *IEEE Transactions on Geoscience and Remote Sensing*, vol. 56, no. 6, pp. 3173–3184, 2018.
- [11] Li, Wei, et al. "Hyperspectral image classification using deep pixel-pair features." *IEEE Transactions on Geoscience and Remote Sensing* 55.2 (2016): 844-853.
- [12] Paoletti, M. E., et al. "A new deep convolutional neural network for fast hyperspectral image classification." *International Society for Photogrammetry and Remote Sensing journal of photogrammetry and remote sensing* 145 (2018): 120-147.
- [13] Wu, Hao, and Saurabh Prasad. "Semi-supervised deep learning using pseudo labels for hyperspectral image classification." *IEEE Transactions on Image Processing* 27.3 (2017): 1259-1270.
- [14] Kaiming He, Xiangyu Zhang, Shaoqing Ren, and Jian Sun, "Deep residual learning for image recognition," in *IEEE International Conference on Computer Vision*, 2016, pp. 770–778.
- [15] Bin Pan, Zhenwei Shi, and Xia Xu, "R-vcanet: A new deep-learning-based hyperspectral image classification method," *IEEE Journal of selected topics in applied earth observations and remote sensing*, vol. 10, no. 5, pp. 1975–1986, 2017.
- [16] Diederik P Kingma and Jimmy Ba, "Adam: A method for stochastic optimization," *arXiv preprint arXiv:1412.6980*, 2014.